# Antigenic landscape analysis of individuals vaccinated with a universal influenza virus vaccine candidate reveals induction of cross-subtype immunity

Philip Meade[1,2], Shirin Strohmeier[2], Maria Carolina Bermúdez-González [2,7], Adolfo García -Sastre[2,3,4,5,6], Peter Palese[2,3], Viviana Simon[2,3,4,5,7], Florian Krammer[1,5,7]*

[1]*Graduate School of Biomedical Sciences, Icahn School of Medicine at Mount Sinai, New York, NY 10029, USA.*
[2]*Department of Microbiology, Icahn School of Medicine at Mount Sinai, New York, NY, United States.*
[3] *Division of Infectious Diseases, Department of Medicine, Icahn School of Medicine at Mount Sinai, New York, NY, United States.*
[4]*Global Health Emerging Pathogens Institute, Icahn School of Medicine at Mount Sinai, New York, NY, United States.*
[5]*Department of Pathology, Molecular and Cell-Based Medicine, Icahn School of Medicine at Mount Sinai, New York, NY, United States.*
[6]*The Tisch Cancer Institute, Icahn School of Medicine at Mount Sinai, New York, NY, United States.*
[7] *Center for Vaccine Research and Pandemic Preparedness (C-VARPP), Icahn School of Medicine at Mount Sinai, New York, NY, USA*

*To whom correspondence should be addressed: florian.krammer@mssm.edu

**Abstract**

Current influenza virus vaccines have to be closely matched to circulating strains to provide good protection and antigenic drift and emerging pandemic influenza virus strains present a difficult challenge for them. Universal influenza virus vaccines, including chimeric hemagglutinin (cHA)-based constructs that target the conserved stalk domain of hemagglutinin, are in clinical development. Due to the conservation of the stalk domain, antibodies directed to it show broad binding profiles, usually within group 1 and group 2 influenza A or influenza B virus phylogenies. However, determining the binding breadth of these antibodies with commonly used immunological methods can be challenging. Here, we analyzed serum samples from a phase I clinical trial (CVIA057, NCT03300050) using an influenza virus protein microarray (IVPM). The IVPM technology allowed us to assess immune responses not only to a large number of group 1 hemagglutinins but also group 2 and influenza B hemagglutinins. In CVIA057, different vaccine modalities including a live attenuated influenza virus vaccine and inactivated influenza virus vaccines with or without adjuvant, all in the context of cHA constructs, were tested. We found that vaccination with adjuvanted, inactivated vaccines induced a very broad antibody response covering group 1 hemagglutinins, with limited induction of antibodies to group 2 hemagglutinins. Our data show that cHA constructs do indeed induce very broad immune responses and that the IVPM technology is a useful tool to measure this breadth that broadly protective or universal influenza virus vaccines aim to induce.

**Importance**

The development of a universal influenza virus vaccine that protects against seasonal drifted, zoonotic or emerging pandemic influenza viruses would be an extremely useful public health tool. Here we test a technology designed to measure the breadth of antibody responses induced by this new class of vaccines.

## Introduction

Seasonal influenza virus vaccines provide narrow protection to circulating strains that are closely matched to the vaccine strains (1-6). Vaccine strains are chosen based on surveillance and prediction (7). When mismatches accrue between vaccine strains and circulating strains – due to unexpected antigenic drift or egg-adaptation of vaccine viruses – the vaccine effectiveness is drastically reduced (1-6). In addition, current seasonal influenza virus vaccines provide negligible protection against emerging pandemic strains. In order to broaden protection from seasonal influenza viruses and to enhance our pandemic preparedness, universal influenza virus vaccines are in development (8, 9). A prominent target for these vaccines is the conserved stalk domain of the hemagglutinin. Antibodies that target this domain can provide broad protection, usually within group 1 HAs (H1, H2, H5, H6, H8, H9, H11, H12, H13, H16, H17, H18) or within group 2 HAs (H3, H4, H7, H10, H14, H15) and occasionally even across groups (10-14).

A chimeric hemagglutinin (cHA) – based candidate universal influenza virus vaccine (15-17) containing a group 1 stalk was recently evaluated in a phase I clinical trial (CVIA 057, clinicaltrials.gov # NCT03300050) (18, 19). In this trial, sequential immunization with cH8/1N1 and cH5/1N1 vaccines was tested. Five groups were evaluated (**Figure 1A**). Group 1 and 2 received an intranasal prime with a cH8/1N1 live attenuated influenza virus vaccine (based on the Leningrad master donor strain (20)) followed by an inactivated cH5/1N1 vaccine with (group 1) and without (group 2) AS03 as adjuvant (21). Group 3 received an adjuvanted inactivated cH8/1N1 vaccine followed by cH5/1N1 adjuvanted inactivated vaccine. Groups 4 and 5 were placebo groups and were analyzed pooled together. When evaluated via enzyme-linked immunosorbent assays (ELISA), antibody induction to the group 1 stalk and H2, H9 and H18 group 1 HAs but not to H3 HA (group 2) was observed (18, 19). Here, we reanalyzed these samples using an influenza virus protein microarray (IVPM), a technology (21, 22) which allowed us to assess binding to a large panel of different hemagglutinins to have a global look at the binding profile of the antibodies induced by this cHA-based group 1 influenza vaccine candidate.

## Results

### Experimental design

We analyzed sera from individuals vaccinated with cH8/1N1 LAIV followed by cH5/1N1 IIV with adjuvant (LAIV8-IIV5/AS03, n=19), cH8/1N1 LAIV followed by cH5/1N1 IIV without adjuvant (LAIV8-IIV5, n=14), cH8/1N1 IIV with AS03 followed by cH5/1N1 with AS03 (IIV8/AS03-IIV5/AS03, n=15) as well as from the pooled placebo groups (Placebo, n=13) (**Figure 1A**). Time points analyzed were day 1 (pre-vaccination), day 29 (28 days post prime), day 85 (pre-boost) and day 113 (28 days post boost). Samples were analyzed using the IVPM platform in a quantitative manner with area under the curve (AUC) measurements of dilution series as readout. The IVPM was designed to contain 21 group 1 HAs covering all subtypes in this group, 13 group 2 HAs covering all subtypes in this group, one influenza B HA, and a cH6/1 HA to measure anti-stalk antibody responses directly (**Table 1**).

### cHA vaccination induces broad group 1 HA IgG responses with high fold-induction across subtypes

First, we analyzed the fold-induction from day 1 to day 28. As previously observed with classical ELISAs (18, 19), vaccination with LAIV (LAIV8-IIV5/AS03 and LAIV8-IIV5 groups) did not induce apparent IgG responses to any group 1 HAs, most likely due to the lack of 'take' of the live attenuated vaccine (18, 19)) (**Figure 1B**). Vaccination with cH8/1N1 inactivated vaccine plus AS03 (IIV8/AS03-IIV5/AS03 group) however induced strong antibody responses to group 1 HAs. The induction appeared to be strongest against non-H1 HAs with slightly lower induction against H1 HAs. This can be explained by higher pre-existing baseline immunity to H1 as compared to other group 1 HAs (see discussion below)

(**Supplemental Figure 1)**. Interestingly, there was also a weak induction of selected group 2 HAs including H4, H10 and H15.

The booster vaccination induced antibodies in all three vaccination groups, with strong induction of group 1 HA reactivity after vaccination with cH5/1N1 with adjuvant (LAIV8-IIV5/AS03, IIV8/AS03-IIV5/AS03) and weaker induction when cH5/1N1 was given without adjuvant (LAIV8-IIV5) (**Figure 1C**). Similar as after vaccination with cH8/1N1 inactivated vaccine with AS03, the induction was strongest against non-H1 group 1 HAs and slightly lower against H1 HAs.

**Aggregate analysis of antibody induction to group 1 and group 2 HAs**

Following this analysis of fold-induction against single HAs, we also performed an aggregate analysis to assess the induction of antibodies to group 1, group 2 and the stalk domain (**Figure 2**). For the analysis of the group 1 stalk response H8 and H5 subtypes were removed since they were also included in the vaccine. After the prime, an induction of antibodies to group 1 HAs was only detected in the group that received the cH8/1N1 inactivated vaccine with AS03 (IIV8/AS03-IIV5/AS03) as already described above. The geometric mean induction for this group post-prime was 10-fold. Titers dropped slightly to day 85 and then increased again to a level of 7.5-fold above baseline post-boost. The group that initially received LAIV and was boosted with inactivated cH5/1N1 AS03 adjuvanted vaccine (LAIV8-IIV5/AS03) reached a 6-fold induction post boost while the non-adjuvanted group (LAIV8-IIV5) reached half that (3-fold). When the stalk-only response was analyzed on the IVPM using a cH6/1 HA the fold-induction basically mirrored the induction seen against group 1 HAs (**Figure 2B**). This aggregate analysis also revealed a slight (2-fold) induction of antibodies to group 2, especially after the prime in the IIV8/AS03-IIV5/AS03 group and after the boost in the LAIV8-IIV5/AS03 group. No induction was found for the placebo control groups.

**Antigenic landscape analysis of the IIV8/AS03-IIV5/AS03 group in comparison to individuals who received seasonal influenza virus vaccine**

Currently, based on the data from CVIA 057, the adjuvanted, inactivated vaccine strategy will move forward into further clinical development. Here, we wanted to take a closer look at the absolute titers induced in individuals vaccinated with the experimental vaccine as compared to the titers observed in individuals who had received the seasonal influenza virus vaccine (QIV), which is currently the standard of care. To do this, we performed an antigenic landscape analysis using multidimensional scaling (22-24). In this analysis, the amino acid sequence difference between antigens is plotted as distance on the x- and y-axis while titers are plotted on the z-axis. Pre-vaccination titers are shown in **Figure 3** as gray planes, post vaccination group 1 titers are shown as blue planes and post-vaccination titers are shown as red planes. No induction of antibodies to group 1 or group 2 HAs was observed in the placebo group (**Figure 3A**). When analyzing responses to QIV, we found a specific but rather low response to both H1 and H3 HAs (which are both included in the vaccine) but induction of antibodies to other group 1 or group 2 HAs was modest to nonexistent (**Figure 3B**). For the IIV8/AS03-IIV5/AS03 groups we analyzed day 29 versus day 1 (**Figure 3C**) and day 113 versus day 1 (**Figure 3D**). In absolute titers, the increase was strongest against members of the H1 clade (H1, H2, H5 and H6) as well as the H9 clade (H8, H9 and H12) and the bat HAs (H17 and H18) at both time points. The rise in absolute titers against the H11 clade (H11, H13 and H16) was lower. As expected, the post-vaccination titers to group 2 HAs did not change much compared to the pre-vaccination titers.

**Discussion**

Universal influenza virus vaccines aim at induction of broadly reactive antibodies that cross HA subtypes (7, 9). Here we use an IVPM, an ideal tool to assess the breadth of antibody responses, to analyze sera from a phase I clinical trial with a group 1 cHA-based universal influenza virus vaccine candidate. This

vaccine was tested in different formulations and was expected to induce broad antibody responses to group 1 HAs (18, 19). It was also expected that little reactivity would be induced to group 2 HAs. This is exactly what we observed in our analysis. Vaccination with inactivated cHA-based vaccines induced strong antibody responses across group 1 HAs, especially when the vaccines were adjuvanted. The response to non-adjuvanted inactivated cHA vaccine was more moderate but detectable. Live attenuated cHA-based vaccines however, did not induce detectable IgG responses in serum. The results reported here are in agreement with the primary analysis of the clinical trial which was conducted using an ELISA methodology (18, 19). However, the more detailed analysis with many HAs on the IVPM allowed us to make additional observations.

Reactivity to the HAs that lend their head domains to the cH8/1 and cH5/1 constructs, labeled H8 and Vn05 H5 in the figure, did not stand out compared to other group 1 HAs. This suggests a stalk-focused rather than a head focused response and is consistent with the absence of a strong head targeting hemagglutination inhibition response against the cH8/1N1 and cH5/1N1 viruses as reported previously (18, 19).

In addition, when fold induction was analyzed, the strongest responses were mounted against non-H1 HAs. This is in contrast to the analysis of absolute titers, where the response to H1 HAs was strongest. This finding can be explained by the much higher baseline titers to H1 HAs. Humans are constantly exposed to H1 viruses via vaccination and infection with seasonal influenza viruses and mount strong anti-head as well as some anti-stalk responses to these HAs. This pre-existing baseline immunity, mostly against the head domain, explains the low fold-induction post cHA vaccination.

Furthermore, we found that absolute titers after cHA vaccinations are not uniform across group 1 HAs. Absolute titers against members of the H1 clade were highest followed by the H9 and bat HA (25, 26) clades. However, absolute titers were lower against the H11 clade. Again, this can be explained by lower baseline titers against members of this clade in general. This is important information and suggests that polyclonal anti-stalk antibodies, while in general being very cross-reactive within a group, may also lose reactivity dependent on phylogenetic distance.

Finally, induction of antibodies against group 2 HAs was also observed. This could be partially due to the induction of pan-HA anti-stalk antibodies which are more rare than group specific antibodies but have been reported (10, 27). However, trimer-interface (TI) antibodies (28-30) that bind to an epitope conserved between head domains across all HA subtypes have been reported to be induced by cHA vaccination as well and may contribute to the cross-group reactivity (19). Both anti-stalk and TI antibodies have been shown to be protective in animal models (14, 28-30) while only anti-stalk antibodies have been established as independent correlate of protection against H1N1 infection so far (31).

In summary, using the IVPM, an innovative new tool for assessment of the breadth of antibody responses, we show that vaccination with cHA-based vaccines induces very broad cross-subtype antibody responses. The vaccine candidate described here is focused on group 1 HAs but constructs for group 2 (32-35) as well as influenza B virus HA (36, 37) are in development. The ultimate goal is it to combine these components in a truly universal trivalent influenza virus vaccine that protects against all seasonal, zoonotic and future pandemic influenza viruses.

## Methods

### Vaccination and clinical trial

Sera were collected from participants of two different IRB approved studies. Samples for Group 1, 2, 3, 4 and 5 were obtained as part of a phase I clinical trial (CVIA 057, clinicaltrials.gov # NCT03300050). This clinical vaccine trial included an LAIV and an IIV vaccine platform. The LAIV expressed the cH8/1 HA, which incorporates an H8 head domain from H8N4 virus A/mallard/Sweden/24/02 and an H1 stalk

domain from the H1N1 virus A/California/04/09 (Cal09), along with the N1 NA of Cal09 in an H1N1 A/Leningrad/134/17/57 backbone, as previously described (38). Meridian Life Sciences in Memphis, Tennessee produced the LAIV in embryonated chicken eggs and formulated it in sterile saline. Two IIV vaccines were used in the clinical trial, including one carrying the cH8/1 HA described above, and one with a cH5/1 HA which incorporates an H5 head domain from the H5N1 virus A/Vietnam/1203/04, and the stalk domain from Cal09. Both IIV vaccines were rescued with Cal09 N1 in the H1N1 A/Puerto Rico/8/34 backbone and were manufactured by GlaxoSmithKline in Dresden, Germany in embryonated chicken eggs as described previously (18, 19).

A $10^{7.5}$ 50% egg infectious dose of cH8/1 LAIV or sterile saline was administered intranasally to vaccinees, who were instructed to clear their noses and lay on their backs and tilt their heads backward. The vaccine or placebo was administered dropwise by needle-less syringe, and vaccinees were instructed to refrain from sneezing during the administration to ensure that the vaccine solution was not expelled. The vaccinations were performed in a containment unit and recipients were required to stay for the next 5 days, or until confirmed to be virus-negative on 3 consecutive days by quantitative RT-PCR. The IIV vaccines or a phosphate-buffered saline (PBS) placebo were administered intramuscularly with an antigen content of 15 µg, in a volume of 0.5 ml in PBS or AS03A.

The trial included three vaccination regimens and two placebo groups, each receiving vaccinations or placebos on day 1 and day 85. Group 1 was the recipient of the cH8/1 LAIV followed by the AS03A-adjuvanted cH5/1 IIV. Group 2 also received the cH8/1 LAIV, then a nonadjuvanted cH5/1 IIV. Group 3 was administered AS03A-adjuvanted cH8/1 IIV and AS03A-adjuvanted cH5/1 IIV. Group 4 constituted the inpatient control group and received saline intranasally in place of the LAIV, then PBS intramuscularly in place of the IIV. Finally, group 5 was the outpatient control group and received two doses of intramuscularly administered PBS. For analysis purposes, the inpatient and outpatient control groups were combined into one placebo group.

Samples from QIV-vaccinated subjects were sourced from an IRB approved observational study which was reviewed and approved by the Mount Sinai Hospital Institutional Review Board (IRB-16-01199). These serum samples were collected prior to seasonal influenza vaccination as well as after 4-6 weeks after vaccination. All participants received the 2018-2019 influenza season vaccine formulations of the Flucelvax (Seqirus) or Fluzone (Sanofi Pasteur) vaccines.

**IVPM and analysis**

IVPMs were produced by printing arrays of recombinant influenza virus HAs onto epoxysilane-coated glass slides (Schott, Mainz, Germany). Each array included 13 HAs diluted in 0.1% milk PBS spotted in triplicate at a volume of 30 nl per spot and a concentration of 100 µg/ml, and each slide contained 24 arrays. After printing, IVPMs were vacuum-packed and stored at -80°C until use. Before use, IVPM slides were allowed to thaw at room temperature, then were removed from their vacuum packaging and incubated at 95-98% relative humidity for two hours to bind the recombinant proteins to the slide surface and inactivate the remaining expoysilane surface of the slides. Afterward, the slides were allowed to dry, and inserted into 96-well gaskets (Arrayit, Sunnyvale, California) and blocked in 3% milk in PBS containing 0.1% Tween 20 (PBS-T) for 90 minutes. The blocking solution was then removed and sera were added at a starting dilution of 1:100 in 1% milk PBS-T at a volume of 100 µl per array, and diluted 1:10 twice across the IVPM slide for 1 hour. After 1 hour, sera were removed and the slides were washed with 220 µl PBS-T three times before being incubated with cy5-labeled secondary antibody diluted 1:1500 in 1% milk PBS-T for one hour. The secondary antibody solution was then removed and slides were washed again with PBST three times, removed from gaskets, rinsed with deionized water and dried with an air compressor. Arrays were then read with a Vidia microarray scanner (Indevr,

Boulder, Colorado), at an exposure time of 1000 ms. AUC was calculated from median fluorescence taking total peak area under 0.04 fluorescence units.

**Recombinant Proteins**

Recombinant HAs were expressed using the baculovirus expression system and consisted of soluble HAs that include trimerization domains and hexahistidine tags. The baculovirus was grown in a Sf9 insect cell line (ATCC CRL-1711), and was used to infect BTI-*TN*-5B1-4 cells for protein production. Secreted recombinant HA was purified with $Ni^{2+}$nitrilotriacetic acid resin columns as described in detail elsewhere (39, 40).

**Multidimensional Scaling**

In order to visualize serum reactivity across different HAs, three-dimensional antibody landscapes were generated (22-24). The horizontal planes in these graphs were generated by assigning *x*-*y* coordinates to HAs derived from a multidimensional scaling analysis of their amino acid sequence differences. The distance between HAs was defined as the number of amino acid differences between HAs in a multiple-sequence alignment. The sum of squared errors between the Euclidean distance in the two-dimensional plane and the HA sequence distance were minimized by the SMACOF algorithm. In each experimental group, HAs were assigned a *z* coordinate equal to their geometric mean AUC values using multilevel B-splines for different time points.

**Statistical analysis and viral sequence analysis**

Graphpad Prism 7.0 was used to calculate geometric means, and to perform Mann-Whitney tests and AUC analyses.

**Acknowledgements**

We thank the study participants for their support of influenza vaccine research efforts. We thank the research team at the Department of Microbiology at the Icahn School of Medicine at Mount Sinai for supporting the development of this vaccine concept since 2011. We also thank the teams at PATH (with special acknowledgement to J.C. Victor, R. Wahid and K. Mahmood), Cincinnati Children's Hospital Medical Center, Duke University, the University of Chicago, GSK, NEOMED-LABS and the EMMES Corporation for their work on this project. Dr. Kimihito Ito of Hokkaido University assisted with generation of our three-dimensional antibody landscape images. The clinical study described was funded in part by the Bill and Melinda Gates Foundation (grant OPP1084518). Basic research leading to this trial was supported by the National Institute of Allergy and Infectious Diseases (NIAID) (grants P01 AI097092, U19 AI109946, R01 AI128821; contracts HHSN26620070010C, HHSN272201400008C, 75N93021C00014). The analysis presented here was funded through the Collaborative Influenza Vaccine Innovation Centers contract (75N93019C00051).

**Conflict of interest statement**

The Icahn School of Medicine at Mount Sinai has filed patent applications regarding universal influenza virus vaccines naming AGC, PP and FK as inventors. AGC, PP and FK have also received royalties and research support for their laboratories from GSK in the past and are currently receiving research support from Dynavax for development of influenza virus vaccines. The A.G.-S. laboratory has also received research support from Pfizer, Senhwa Biosciences, Kenall Manufacturing, Avimex, Johnson & Johnson, 7Hills Pharma, Pharmamar, ImmunityBio, Accurius, Nanocomposix, Hexamer, N-fold LLC, Model Medicines, Atea Pharma, Applied Biological Laboratories and Merck, outside of the reported work. A.G.-S. has consulting agreements for the following companies involving cash and/or stock: Vivaldi Biosciences, Contrafect, 7Hills Pharma, Avimex, Vaxalto, Pagoda, Accurius, Esperovax, Farmak, Applied

Biological Laboratories, Pharmamar, Paratus, CureLab Oncology, CureLab Veterinary, Synairgen and Pfizer, outside of the reported work. A.G.-S. has been an invited speaker in meeting events organized by Seqirus, Janssen and Astrazeneca.

**References**

1. Chambers BS, Parkhouse K, Ross TM, Alby K, Hensley SE. 2015. Identification of Hemagglutinin Residues Responsible for H3N2 Antigenic Drift during the 2014-2015 Influenza Season. Cell Rep 12:1-6.
2. de Jong JC, Beyer WE, Palache AM, Rimmelzwaan GF, Osterhaus AD. 2000. Mismatch between the 1997/1998 influenza vaccine and the major epidemic A(H3N2) virus strain as the cause of an inadequate vaccine-induced antibody response to this strain in the elderly. J Med Virol 61:94-9.
3. Heikkinen T, Ikonen N, Ziegler T. 2014. Impact of influenza B lineage-level mismatch between trivalent seasonal influenza vaccines and circulating viruses, 1999-2012. Clin Infect Dis 59:1519-24.
4. Skowronski DM, Janjua NZ, De Serres G, Sabaiduc S, Eshaghi A, Dickinson JA, Fonseca K, Winter AL, Gubbay JB, Krajden M, Petric M, Charest H, Bastien N, Kwindt TL, Mahmud SM, Van Caeseele P, Li Y. 2014. Low 2012-13 influenza vaccine effectiveness associated with mutation in the egg-adapted H3N2 vaccine strain not antigenic drift in circulating viruses. PLoS One 9:e92153.
5. Skowronski DM, Sabaiduc S, Leir S, Rose C, Zou M, Murti M, Dickinson JA, Olsha R, Gubbay JB, Croxen MA, Charest H, Bastien N, Li Y, Jassem A, Krajden M, De Serres G. 2019. Paradoxical clade- and age-specific vaccine effectiveness during the 2018/19 influenza A(H3N2) epidemic in Canada: potential imprint-regulated effect of vaccine (I-REV). Euro Surveill 24.
6. Xie H, Wan XF, Ye Z, Plant EP, Zhao Y, Xu Y, Li X, Finch C, Zhao N, Kawano T, Zoueva O, Chiang MJ, Jing X, Lin Z, Zhang A, Zhu Y. 2015. H3N2 Mismatch of 2014-15 Northern Hemisphere Influenza Vaccines and Head-to-head Comparison between Human and Ferret Antisera derived Antigenic Maps. Sci Rep 5:15279.
7. Gerdil C. 2003. The annual production cycle for influenza vaccine. Vaccine 21:1776-9.
8. Nachbagauer R, Krammer F. 2017. Universal influenza virus vaccines and therapeutic antibodies. Clin Microbiol Infect 23:222-228.
9. Berlanda Scorza F, Tsvetnitsky V, Donnelly JJ. 2016. Universal influenza vaccines: Shifting to better vaccines. Vaccine 34:2926-2933.
10. Dreyfus C, Laursen NS, Kwaks T, Zuijdgeest D, Khayat R, Ekiert DC, Lee JH, Metlagel Z, Bujny MV, Jongeneelen M, van der Vlugt R, Lamrani M, Korse HJ, Geelen E, Sahin Ö, Sieuwerts M, Brakenhoff JP, Vogels R, Li OT, Poon LL, Peiris M, Koudstaal W, Ward AB, Wilson IA, Goudsmit J, Friesen RH. 2012. Highly conserved protective epitopes on influenza B viruses. Science 337:1343-8.
11. Friesen RH, Lee PS, Stoop EJ, Hoffman RM, Ekiert DC, Bhabha G, Yu W, Juraszek J, Koudstaal W, Jongeneelen M, Korse HJ, Ophorst C, Brinkman-van der Linden EC, Throsby M, Kwakkenbos MJ, Bakker AQ, Beaumont T, Spits H, Kwaks T, Vogels R, Ward AB, Goudsmit J, Wilson IA. 2014. A common solution to group 2 influenza virus neutralization. Proc Natl Acad Sci U S A 111:445-50.
12. Ekiert DC, Bhabha G, Elsliger MA, Friesen RH, Jongeneelen M, Throsby M, Goudsmit J, Wilson IA. 2009. Antibody recognition of a highly conserved influenza virus epitope. Science 324:246-51.
13. Corti D, Voss J, Gamblin SJ, Codoni G, Macagno A, Jarrossay D, Vachieri SG, Pinna D, Minola A, Vanzetta F, Silacci C, Fernandez-Rodriguez BM, Agatic G, Bianchi S, Giacchetto-Sasselli I, Calder L, Sallusto F, Collins P, Haire LF, Temperton N, Langedijk JP, Skehel JJ, Lanzavecchia A. 2011. A neutralizing antibody selected from plasma cells that binds to group 1 and group 2 influenza A hemagglutinins. Science 333:850-6.

14. Wu NC, Wilson IA. 2018. Structural insights into the design of novel anti-influenza therapies. Nat Struct Mol Biol 25:115-121.
15. Hai R, Krammer F, Tan GS, Pica N, Eggink D, Maamary J, Margine I, Albrecht RA, Palese P. 2012. Influenza viruses expressing chimeric hemagglutinins: globular head and stalk domains derived from different subtypes. J Virol 86:5774-81.
16. Krammer F, Pica N, Hai R, Margine I, Palese P. 2013. Chimeric hemagglutinin influenza virus vaccine constructs elicit broadly protective stalk-specific antibodies. J Virol 87:6542-50.
17. Chen CJ, Ermler ME, Tan GS, Krammer F, Palese P, Hai R. 2016. Influenza A Viruses Expressing Intra- or Intergroup Chimeric Hemagglutinins. J Virol 90:3789-93.
18. Bernstein DI, Guptill J, Naficy A, Nachbagauer R, Berlanda-Scorza F, Feser J, Wilson PC, Solórzano A, Van der Wielen M, Walter EB, Albrecht RA, Buschle KN, Chen YQ, Claeys C, Dickey M, Dugan HL, Ermler ME, Freeman D, Gao M, Gast C, Guthmiller JJ, Hai R, Henry C, Lan LY, McNeal M, Palm AE, Shaw DG, Stamper CT, Sun W, Sutton V, Tepora ME, Wahid R, Wenzel H, Wohlbold TJ, Innis BL, García-Sastre A, Palese P, Krammer F. 2020. Immunogenicity of chimeric haemagglutinin-based, universal influenza virus vaccine candidates: interim results of a randomised, placebo-controlled, phase 1 clinical trial. Lancet Infect Dis 20:80-91.
19. Nachbagauer R, Feser J, Naficy A, Bernstein DI, Guptill J, Walter EB, Berlanda-Scorza F, Stadlbauer D, Wilson PC, Aydillo T, Behzadi MA, Bhavsar D, Bliss C, Capuano C, Carreño JM, Chromikova V, Claeys C, Coughlan L, Freyn AW, Gast C, Javier A, Jiang K, Mariottini C, McMahon M, McNeal M, Solórzano A, Strohmeier S, Sun W, Van der Wielen M, Innis BL, García-Sastre A, Palese P, Krammer F. 2021. A chimeric hemagglutinin-based universal influenza virus vaccine approach induces broad and long-lasting immunity in a randomized, placebo-controlled phase I trial. Nat Med 27:106-114.
20. Isakova-Sivak I, Chen LM, Matsuoka Y, Voeten JT, Kiseleva I, Heldens JG, den Bosch H, Klimov A, Rudenko L, Cox NJ, Donis RO. 2011. Genetic bases of the temperature-sensitive phenotype of a master donor virus used in live attenuated influenza vaccines: A/Leningrad/134/17/57 (H2N2). Virology 412:297-305.
21. Meade P, Latorre-Margalef N, Stallknecht DE, Krammer F. 2017. Development of an influenza virus protein microarray to measure the humoral response to influenza virus infection in mallards. Emerg Microbes Infect 6:e110.
22. Meade P, Kuan G, Strohmeier S, Maier HE, Amanat F, Balmaseda A, Ito K, Kirkpatrick E, Javier A, Gresh L, Nachbagauer R, Gordon A, Krammer F. 2020. Influenza Virus Infection Induces a Narrow Antibody Response in Children but a Broad Recall Response in Adults. mBio 11.
23. Nachbagauer R, Choi A, Hirsh A, Margine I, Iida S, Barrera A, Ferres M, Albrecht RA, García-Sastre A, Bouvier NM, Ito K, Medina RA, Palese P, Krammer F. 2017. Defining the antibody cross-reactome directed against the influenza virus surface glycoproteins. Nat Immunol 18:464-473.
24. Ito K, Igarashi M, Miyazaki Y, Murakami T, Iida S, Kida H, Takada A. 2011. Gnarled-trunk evolutionary model of influenza A virus hemagglutinin. PLoS One 6:e25953.
25. Tong S, Li Y, Rivailler P, Conrardy C, Castillo DA, Chen LM, Recuenco S, Ellison JA, Davis CT, York IA, Turmelle AS, Moran D, Rogers S, Shi M, Tao Y, Weil MR, Tang K, Rowe LA, Sammons S, Xu X, Frace M, Lindblade KA, Cox NJ, Anderson LJ, Rupprecht CE, Donis RO. 2012. A distinct lineage of influenza A virus from bats. Proc Natl Acad Sci U S A 109:4269-74.
26. Tong S, Zhu X, Li Y, Shi M, Zhang J, Bourgeois M, Yang H, Chen X, Recuenco S, Gomez J, Chen LM, Johnson A, Tao Y, Dreyfus C, Yu W, McBride R, Carney PJ, Gilbert AT, Chang J, Guo Z, Davis CT, Paulson JC, Stevens J, Rupprecht CE, Holmes EC, Wilson IA, Donis RO. 2013. New world bats harbor diverse influenza A viruses. PLoS Pathog 9:e1003657.
27. Corti D, Voss J, Gamblin SJ, Codoni G, Macagno A, Jarrossay D, Vachieri SG, Pinna D, Minola A, Vanzetta F, Silacci C, Fernandez-Rodriguez BM, Agatic G, Bianchi S, Giacchetto-Sasselli I, Calder L,

Sallusto F, Collins P, Haire LF, Temperton N, Langedijk JP, Skehel JJ, Lanzavecchia A. 2011. A neutralizing antibody selected from plasma cells that binds to group 1 and group 2 influenza A hemagglutinins. Science 333:850-6.

28. Lee J, Boutz DR, Chromikova V, Joyce MG, Vollmers C, Leung K, Horton AP, DeKosky BJ, Lee CH, Lavinder JJ, Murrin EM, Chrysostomou C, Hoi KH, Tsybovsky Y, Thomas PV, Druz A, Zhang B, Zhang Y, Wang L, Kong WP, Park D, Popova LI, Dekker CL, Davis MM, Carter CE, Ross TM, Ellington AD, Wilson PC, Marcotte EM, Mascola JR, Ippolito GC, Krammer F, Quake SR, Kwong PD, Georgiou G. 2016. Molecular-level analysis of the serum antibody repertoire in young adults before and after seasonal influenza vaccination. Nat Med 22:1456-1464.

29. Bangaru S, Lang S, Schotsaert M, Vanderven HA, Zhu X, Kose N, Bombardi R, Finn JA, Kent SJ, Gilchuk P, Gilchuk I, Turner HL, García-Sastre A, Li S, Ward AB, Wilson IA, Crowe JE. 2019. A Site of Vulnerability on the Influenza Virus Hemagglutinin Head Domain Trimer Interface. Cell 177:1136-1152.e18.

30. Watanabe A, McCarthy KR, Kuraoka M, Schmidt AG, Adachi Y, Onodera T, Tonouchi K, Caradonna TM, Bajic G, Song S, McGee CE, Sempowski GD, Feng F, Urick P, Kepler TB, Takahashi Y, Harrison SC, Kelsoe G. 2019. Antibodies to a Conserved Influenza Head Interface Epitope Protect by an IgG Subtype-Dependent Mechanism. Cell 177:1124-1135.e16.

31. Ng S, Nachbagauer R, Balmaseda A, Stadlbauer D, Ojeda S, Patel M, Rajabhathor A, Lopez R, Guglia AF, Sanchez N, Amanat F, Gresh L, Kuan G, Krammer F, Gordon A. 2019. Novel correlates of protection against pandemic H1N1 influenza A virus infection. Nat Med 25:962-967.

32. Margine I, Krammer F, Hai R, Heaton NS, Tan GS, Andrews SA, Runstadler JA, Wilson PC, Albrecht RA, García-Sastre A, Palese P. 2013. Hemagglutinin stalk-based universal vaccine constructs protect against group 2 influenza A viruses. J Virol 87:10435-46.

33. Asthagiri Arunkumar G, McMahon M, Pavot V, Aramouni M, Ioannou A, Lambe T, Gilbert S, Krammer F. 2019. Vaccination with viral vectors expressing NP, M1 and chimeric hemagglutinin induces broad protection against influenza virus challenge in mice. Vaccine 37:5567-5577.

34. McMahon M, Asthagiri Arunkumar G, Liu WC, Stadlbauer D, Albrecht RA, Pavot V, Aramouni M, Lambe T, Gilbert SC, Krammer F. 2019. Vaccination With Viral Vectors Expressing Chimeric Hemagglutinin, NP and M1 Antigens Protects Ferrets Against Influenza Virus Challenge. Front Immunol 10:2005.

35. Krammer F, Margine I, Hai R, Flood A, Hirsh A, Tsvetnitsky V, Chen D, Palese P. 2014. H3 stalk-based chimeric hemagglutinin influenza virus constructs protect mice from H7N9 challenge. J Virol 88:2340-3.

36. Ermler ME, Kirkpatrick E, Sun W, Hai R, Amanat F, Chromikova V, Palese P, Krammer F. 2017. Chimeric Hemagglutinin Constructs Induce Broad Protection against Influenza B Virus Challenge in the Mouse Model. J Virol 91.

37. Sun W, Kirkpatrick E, Ermler M, Nachbagauer R, Broecker F, Krammer F, Palese P. 2019. Development of Influenza B Universal Vaccine Candidates Using the "Mosaic" Hemagglutinin Approach. J Virol 93.

38. Nachbagauer R, Liu W-C, Choi A, Wohlbold TJ, Atlas T, Rajendran M, Solórzano A, Berlanda-Scorza F, García-Sastre A, Palese P, Albrecht RA, Krammer F. 2017. A universal influenza virus vaccine candidate confers protection against pandemic H1N1 infection in preclinical ferret studies. npj Vaccines 2:26.

39. Krammer F, Margine I, Tan GS, Pica N, Krause JC, Palese P. 2012. A carboxy-terminal trimerization domain stabilizes conformational epitopes on the stalk domain of soluble recombinant hemagglutinin substrates. PLoS One 7:e43603.

40. Margine I, Palese P, Krammer F. 2013. Expression of functional recombinant hemagglutinin and neuraminidase proteins from the novel H7N9 influenza virus using the baculovirus expression system. J Vis Exp:e51112.

## Tables

**Table 1: Recombinant HAs**

| HA | Virus from which the recombinant HA was derived |
|---|---|
| **Group 1 HAs** | |
| Mich15 H1 | A/Michigan/45/15 (H1N1) |
| Cal09 H1 | A/California/04/09 (H1N1) |
| NC99 H1 | A/New Caledonia/20/99 (H1N1) |
| Tex91 H1 | A/Texas/36/91 (H1N1) |
| USSR77 H1 | A/USSR/1977 (H1N1) |
| Denv57 H1 | A/Denver/1/57 (H1N1) |
| PR34 H1 | A/Puerto Rico/8/34 (H1N1) |
| H2 | A/Japan/305/57 (H2N2) |
| Pintail H5 | A/Northern Pintail/WA/40964/2014 (H5N2) |
| Indo04 H5 | A/Indonesia/05/2005 (H5N1) |
| Shz16 H5 | A/Shenzen/1/16 (H5N1) |
| Vn04 H5 | A/Vietnam/1203/04 (H5N1) |
| H6 | A/Taiwan/2/13 (H6N1) |
| H11 | A/shoveler/Netherlands/18/99 (H11N7) |
| H13 | A/black headed gull/Sweden/1/99 (H13N6) |
| H16 | A/black headed gull/Sweden/5/99 (H16N3) |
| H8 | A/mallard/Sweden/24/02 (H8N4) |
| H12 | A/mallard/Interior Alaska/7MP0167/07 (H12N5) |
| H9 | A/guinea fowl/Hong Kong/WF10/1999 (H9N2) |
| H17 | A/yellow shouldered bat/Guatemala/06/10 (H17N10) |
| H18 | A/bat/Peru/33/10 (H18N11) |
| **Group 2 HAs** | |
| Sing16 H3 | A/Singapore/INFIMH-16-0019/2016 (H3N2) |
| Switz13 H3 | A/Switzerland/9715293/2013 (H3N2) |
| Perth09 H3 | A/Perth/16/2009 (H3N2) |
| Wisc05 H3 | A/Wisconsin/67/2005 (H3N2) |
| Wyo03 H3 | A/Wyoming/3/2003 (H3N2) |
| Panama99 H3 | A/Panama/2007/1999 (H3N2) |
| Phil82 H3 | A/Philippines/2/82 (H3N2) |
| H3V | A/Indiana/10/11 (H3N2) |
| H4 | A/duck/Czech/56 (H4N6) |
| H14 | A/mallard/Gurjev/263/82 (H14N5) |
| H7 | A/Hong Kong/2014/2017 (H7N9) |
| H10 | A/mallard/Interior Alaska/10BM01929/10 (H10N7) |
| H15 | A/shearwater/West Australia/2576/79 (H15N9) |
| **Influenza B HA** | |
| B/Wisc HA | B/Wisconsin/1/2010 (B-HA) |

## Figure legends

**Figure 1. Geometric means of serum IgG induction against influenza virus HAs by experimental group** **(A)** Experimental overview. **(B)** Fold induction from day 1 to day 29. **(C)** Fold induction from day 1 to day 113.

**Figure 2. Geometric means of serum IgG induction against HA groups** Heterologous group 1 HAs **(A)** were defined as non H1, H8, and H5 HAs belonging to group 1. **(B)** Induction against cH6/1. **(C)** induction against group 2 HAs. Geometric means with 95% confidence intervals shown. Significant differences from placebo group were determined by Mann-Whitney tests. * $P$ <0.05.

**Figure 3 IgG antigenic landscapes of vaccinees pre- and post-vaccination** Influenza virus protein microarray (IVPM) AUC values and amino acid sequences were used to generate antigenic landscapes using multidimensional scaling. The x and y axes represent amino acid differences between HAs used as the substrate and the z axis represents AUC from geometric mean titers, showing IgG binding to HAs. The gray plane underneath the red and blue planes represents the pre-vaccination reactivity, and the blue plane and red plane represent the post-vaccination group 1 reactivity and group 2 reactivity, respectively. The different strains/subtypes are indicated by colored spheres labeled with the HA name. **(A)** Placebo group, **(B)** QIV group, **(C)** IIV8/AS03-IIV5/AS03 group, days 1-29, **(D)** IIV8/AS03-IIV5/AS03 group, days 1-113.

**Supplemental Figure 1 IgG titers of vaccinees against influenza virus A protein panel** Influenza virus protein microarray (IVPM) AUC values and geometric means to HAs shown for experimental groups at each time point. **(A-D)** LAIV8-IIV5/AS03, **(E-H)** LAIV8-IIV5, **(I-L)** IIIV8/AS03-IIV5/AS03, **(M-P)** placebo group.

A


| Group | Dose 1 | Dose 2 |
|---|---|---|
| LAIV8-IIV5/AS03 | cH8/1N1 LAIV | cH5/1N1 IIV + AS03 |
| LAIV8/IIV5 | cH8/1N1 LAIV | cH5/1N1 IIV |
| IIV8/AS03 - IIV5/AS03 | cH8/1N1 IIV + AS03 | cH5/1N1 IIV + AS03 |
| Saline-PBS | Saline | PBS |
| PBS-PBS | PBS | PBS |


B

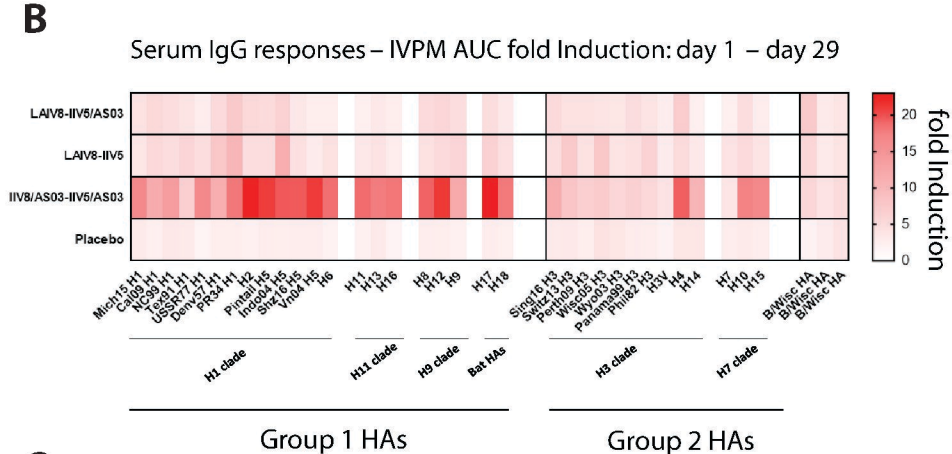


C

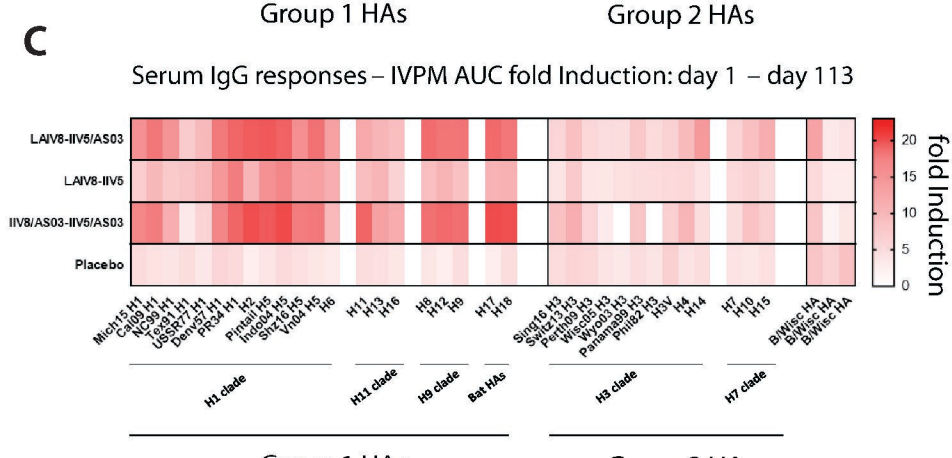

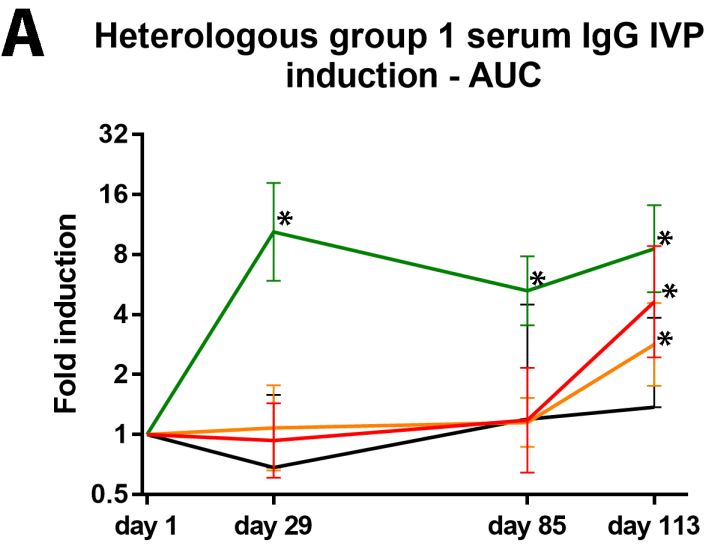


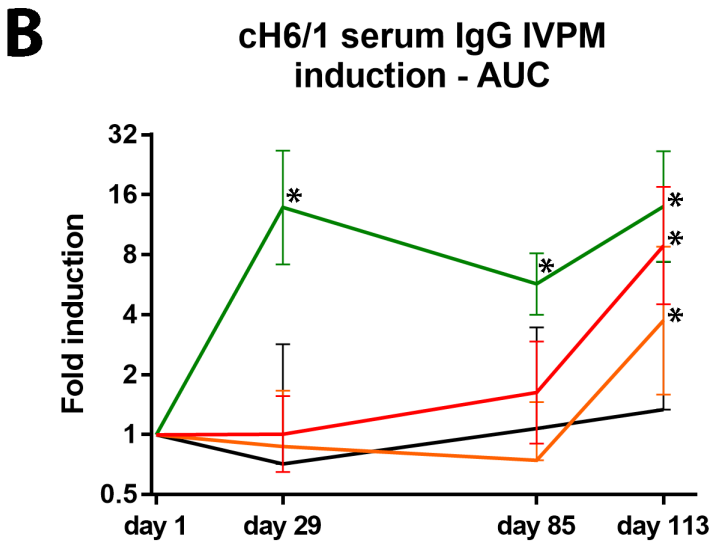


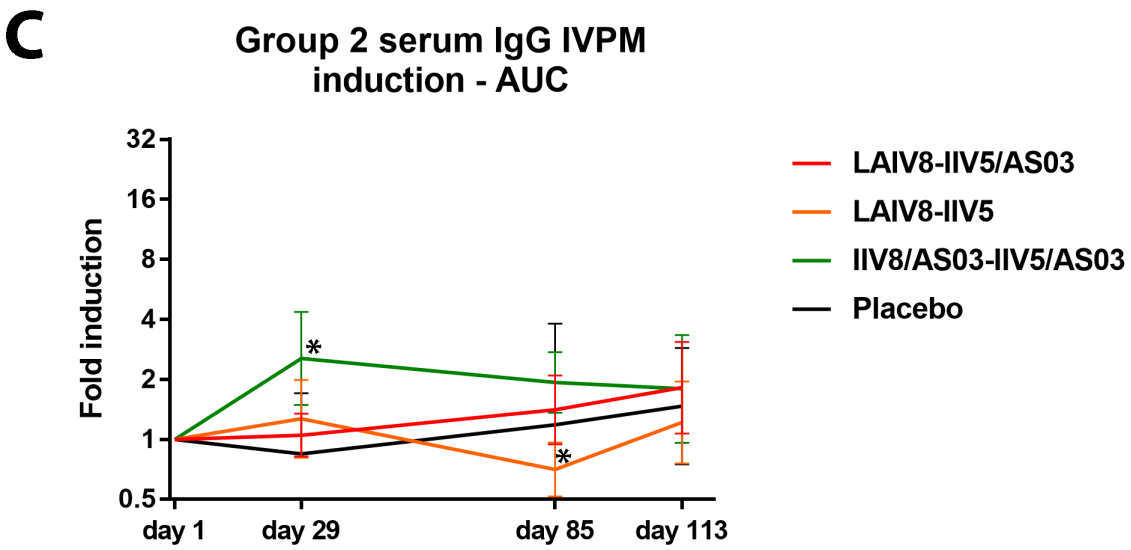

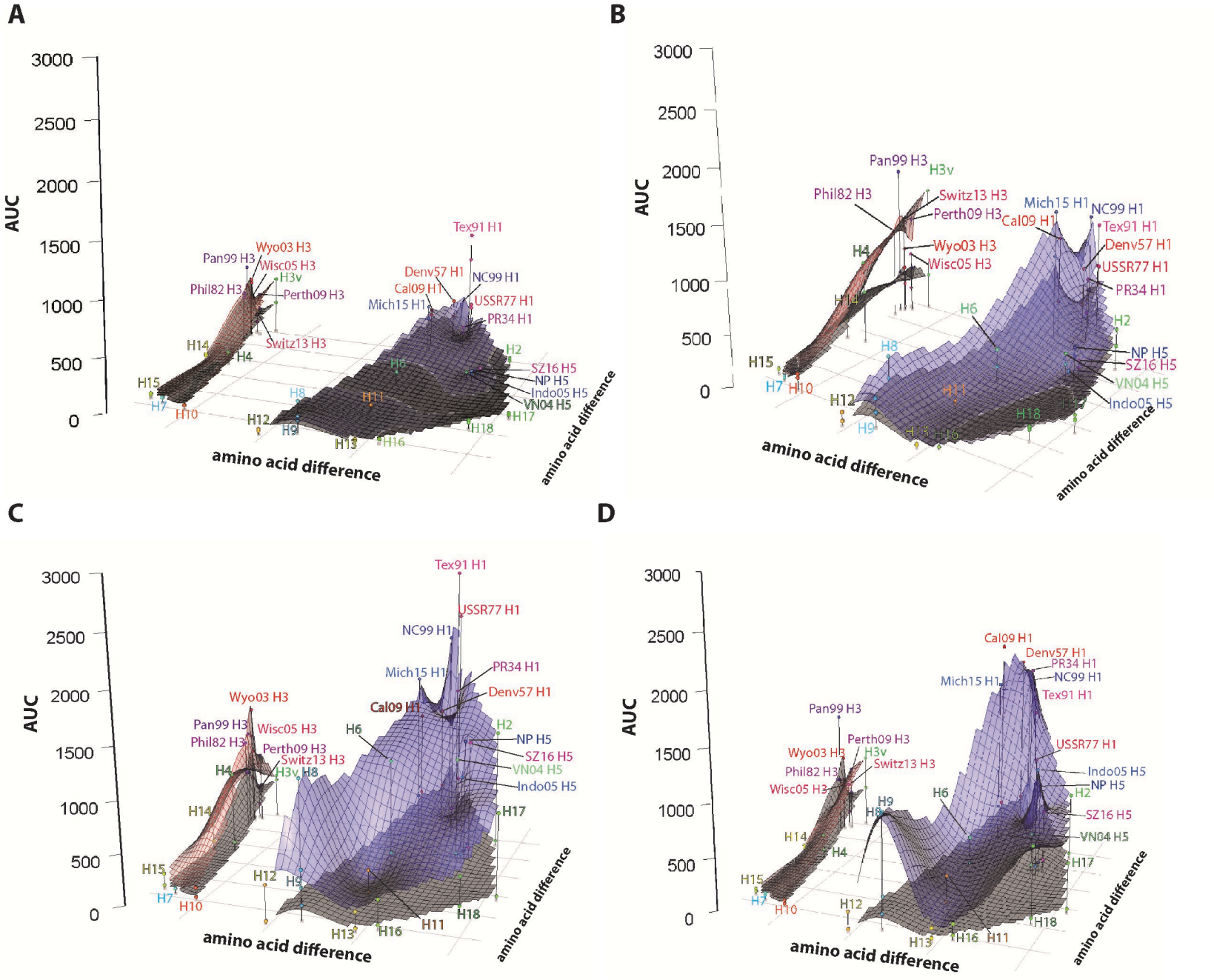
A
B
C
D
AUC
3000
2500
2000
1500
1000
500
0
amino acid difference
Wyo03 H3
Pan99 H3
Wisc05 H3
H3v
Phil82 H3
Perth09 H3
Switz13 H3
H14
H4
H15
H7
H10
H8
H12
H9
H13
H16
H11
H18
H17
H6
H2
NP H5
SZ16 H5
VN04 H5
Indo05 H5
Tex91 H1
Denv57 H1
NC99 H1
Cal09 H1
Mich15 H1
USSR77 H1
PR34 H1